ELSEVIER

Journal of Biomechanics 34 (2001) 765–772

JOURNAL OF BIOMECHANICS

www.elsevier.com/locate/jbiomech
www.JBiomech.com

Theoretical analysis of shape transformation of V-79 cells after treatment with cytochalasin B

Aleš Iglič[a,*], Peter Veranič[b], Urška Batista[c], Veronika Kralj-Iglič[c]

[a] *Laboratory of Applied Physics, Faculty of Electrical Engineering, University of Ljubljana, Tražaška 25, SI-1000 Ljubljana, Slovenia*
[b] *Institute of Cell Biology, Faculty of Medicine, University of Ljubljana, SI-1000, Ljubljana, Slovenia*
[c] *Faculty of Medicine, University of Ljubljana, Vrazov trg 3 SI-1000 Ljubljana, Slovenia*

Accepted 15 January 2001

Abstract

We observed that after treatment of V-79 fibroblasts with cytochalasin B the area of cell contact with the substrate is essentially reduced, the microtubules are organized into rodlike structures and the actin filaments are disintegrated. Remnants of the actin cortex become concentrated in the form of discrete patches under the plasma membrane. The described changes in the organization of the cytoskeleton and of the cortical shell are accompanied by the formation of a cell shape resembling the Greek letter ϕ. We calculated that the ϕ shape corresponds to the minimum of the stretching energy of the cortical shell at relevant geometrical constraints. In line with this result, if cytochalasin B treatment was followed by colchicine application which disrupted the microtubular rod, the characteristic ϕ shape completely disappeared. This study suggests that the effect of the microtubular rod on the cell shape can be theoretically well described by taking into account some basic conditions for the mechanical equlibrium of the cell cortical shell and the appropriate geometrical constraints.

Keywords: Cell shape; Cytoskeleton; Elastic energy; Cortical shell; Vesiculation

1. Introduction

Changes in the cell shapes are the result of the changes in the organization of the cytoskeleton (Gupta et al., 1996; Boulbitch, 1998) and of the cortical shell (Yeung and Evans, 1989; Evans and Skalak, 1980). The cytoskeleton is the network consisting of three main types of protein filaments: the microtubules, the actin filaments and the intermediate filaments which are acting in cooperation with each other (Alberts et al., 1994). Based on ultrastructure evidence, the cortical shell encircling most eucariotic cells is a system built up of a superficial plasma membrane and a subsurface gel-like actin cortex layer (Evans and Kukan, 1984; Yeung and Evans, 1989).

In this study, we investigated the influence of the change in configuration of the microtubules and the actin filaments on the change of the shapes of V-79 cells due to treatment with cytochalasin B and colchicine. The experimental results are compared to the theoretical predictions in order to elucidate the possible physical mechanisms leading to the observed cell shapes.

2. Materials and methods

2.1. Cells

The V-79-379A cells (diploid lung fibroblasts of Chinese hamster) were grown in Eagle MEM (minimal essential medium) supplemented with 10% fetal calf serum (FCS), penicillin (100 U/ml) and streptomycin (100 mg/ml) at 37°C in a incubator with 5% CO_2 atmosphere. The cells (2×10^5) were seeded in 50 mm plastic Petri dishes. After 24 h cells were treated with cytochalasin B (stock solution 1 mg/1 ml in DMSO, final concentration of 2 μmol/l in culture medium) for 1 h, and then also with colchicine (stock solution 100 μmol/l in PBS, final concentration of 1 μmol/l in culture medium) for 1 h.

*Corresponding author. Tel.: +386-1-4250-278; fax: +386-1-4264-630.
E-mail address: ales.iglic@fe.uni-lj.si (A. Iglič).

0021-9290/01/$ - see front matter
PII: S0021-9290(01)00016-1

2.2. Scanning microscopy

The cells grown on round cover slides were fixed in 2% paraformaldehyde and 2% glutaraldehyde in 0.1 M phosphate buffer (pH 7.4) for 3–4 h at 4°C. The tissue samples were rinsed in 0.1 M cacodylate buffer and postfixed in buffered 1% osmium tetroxide for 1 h at 4°C. Specimens were critical point dried, and sputter-coated with gold. The cells were examined at 15 kV with a scanning electron microscope (Jeol JSM 84A).

2.3. Tubulin staining

The cells were simultaneously fixed and extracted with a mixture of 4% formaldehyde, microtubule stabilizing buffer prepared as described by Bell and Safiejko-Mroczka (1995) and 0.5% Triton at 37°C for 30 min. After washing in PBS and blocking of unspecific labelling with 1% BSA, the cells were immunolabelled with monoclonal anti β-tubulin (SIGMA) over night. The FITC-labelled secondary antibodies (SIGMA) were applied for 2 h at 37°C. After washing, the cells were mounted in vectashield or vectashield with DAPI (Vector) and examined in fluorescent microscope (LEITZ Laborlux S).

2.4. Actin staining

The labelling of actin was done as a modified procedure of Bell and Safiejko-Mroczka (1995). The cells were fixed in buffered 4% formaldehyde for 1 h. After rinsing in PBS, the cells were labelled with TRITC-phalloidin (1.6 μM; Sigma) containing 20% methanol for 1 h. After washing, the cells were mounted in vectashield or vectashield with DAPI (Vector) and examined in fluorescent microscope (LEITZ Laborlux S).

3. Experimental results

In normal culture conditions the V-79 fibroblasts are flat cells bound to the substrate and mainly spreading in one direction with the cell surface structured into microspikes (Fig. 1a). The microtubules in these cells are oriented radially toward the cell surface (Fig. 2a) while the actin filaments are organized into parallel stress fibers aligned along the long axis of the cell. At the cortical shell there is a distinct layer of actin cortex attached to the inner side of the plasma membrane (Fig. 3a).

After cytochalasin B treatment the cell body reduced the area of contact with the substrate and became globular. Majority of the cells exibited two long cylindrical protrusions pointing to the opposite directions, so that the cells resembled the ϕ shape (Fig. 1b). The surface of these protrusions was smooth with less microspikes compared to the cell body. The immunofluorescence labelling demonstrated that the microtubules were concentrated in these cylindrical protrusions and organized into rodlike structures (Fig. 2b). The nucleus was located laterally in the cell body. In contrast, the mitotic cells did not form any protrusions after the cytochalasin B treatment while their mitotic spindle was well preserved (Fig. 2b).

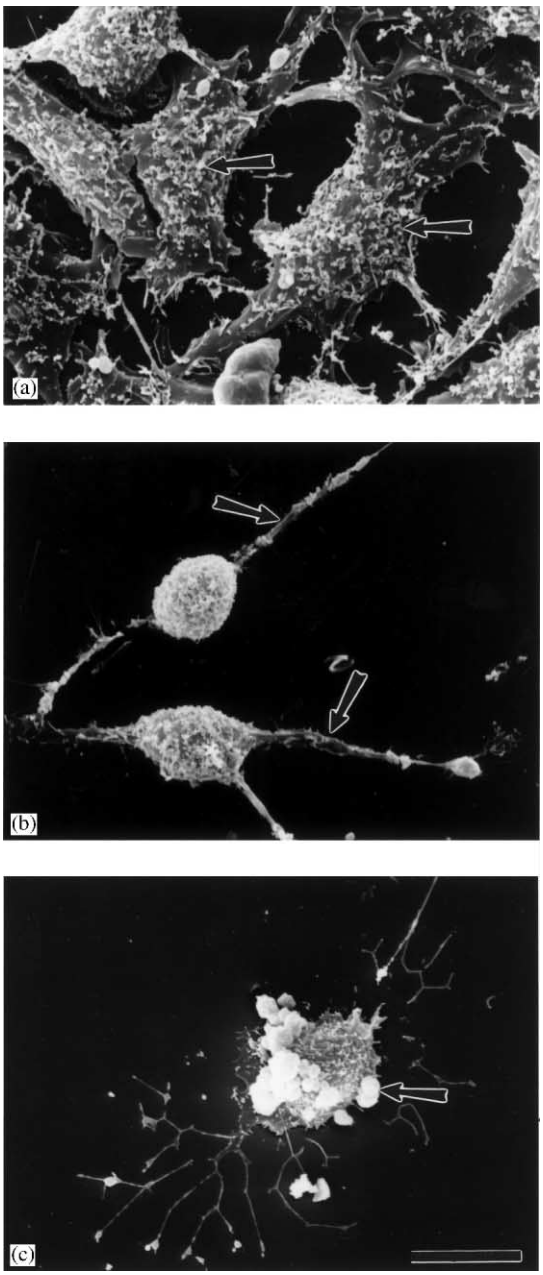

Fig. 1. (a) In untreated V79 cells, numerous microspikes are observed on the cell surface (↑) with scanning microscope; (b) cells treated with the cytochalasin B are ϕ shaped with majority of microspikes on globular cell body and minority on cylindrical protrusions (↑); (c) on cells treated with the cytochalasin B and colchicine, large vesicles are attached to the cell body. Bar = 10 μm.

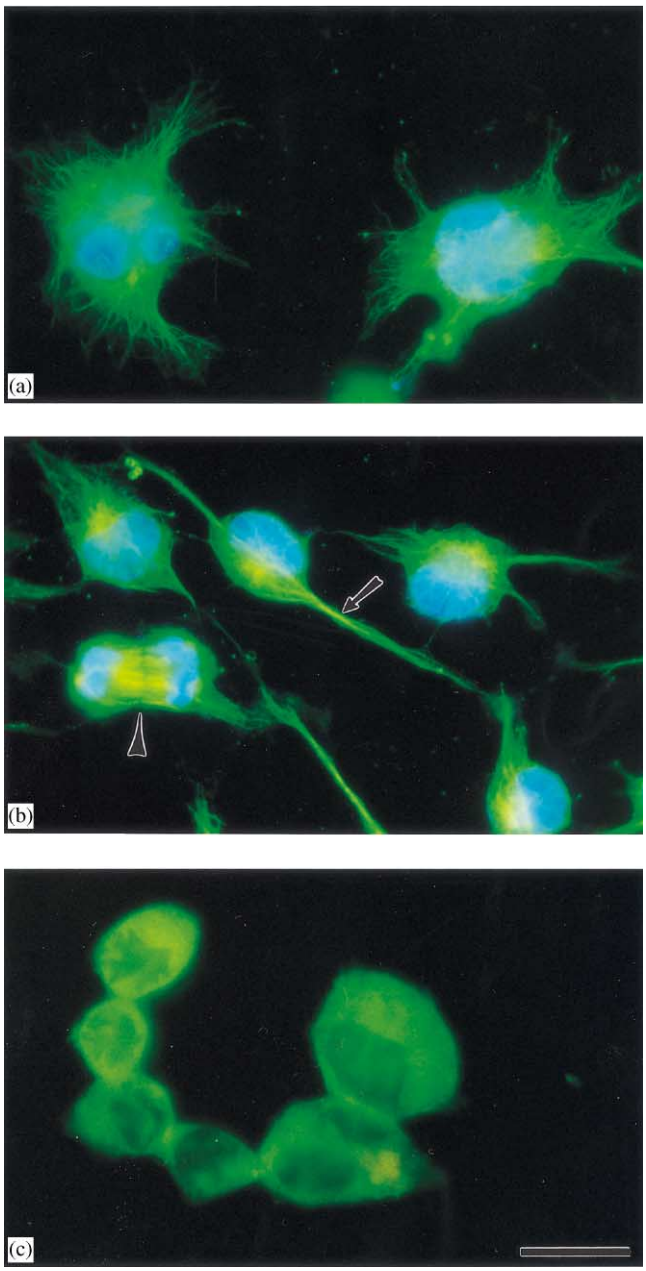

Fig. 2. (a) In the untreated cells, the microtubules labelled with FITC (green) are radially oriented and the nucleus labelled with DAPI (blue) is at the center; (b) after the treatment with the cytochalasin B the parallel microtubules are concentrated in cylindrical protrusions (↑). The mitotic cell is marked by the arrowhead. The nucleus is labelled with DAPI; (c) diffusely dispersed tubulin in rounded cells treated with cytochalasin B and colchicine. Bar = 10 μm.

Even more dramatic changes after the treatment with cytochalasin B were found on actin filaments. The stress fibers were disintegrated and the remnants of the actin cortex became concentrated in the form of discrete pathches under the plasma membrane of the cell body. Within the protrusions, small fragments of actin filaments could be observed (Fig. 3b).

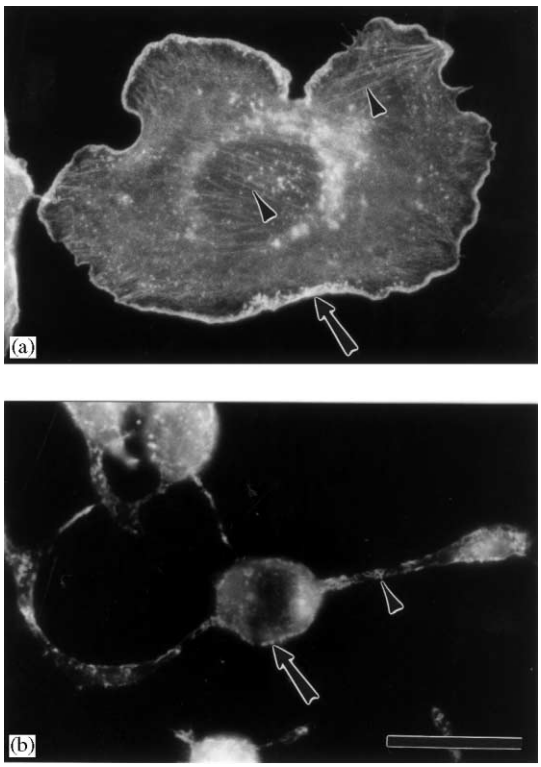

Fig. 3. (a) In the untreated cells, the actin is organized in a thick cortex (arrowhead) close to the plasma membrane and into parallel stress fibers (↑); (b) after the treatment with the cytochalasin B the disintegrated actin filaments are found at the plasma membrane within cell body (↑) and in the long protrusions (arrowhead). Bar = 10 μm.

In the cells, where the cytochalasin B treatment was followed by a subsequent colchicine application, the tubular protrusions disappeared, while the cells were covered with many spherical exovesicles (Fig. 1c). The microtubules were completely disorganized and the tubulin was diffusely spread in the cytoplasm (Fig. 2c).

4. Theoretical description

It was shown that cytochalasin B treatment of V-79 fibroblasts induces a large reduction of the contact area of the cell with the substrate, disaggregation of the actin filaments and reorganization of the microtubules into a rodlike structure. Hence, after cytochalasin B treatment, the shape of V-79 cell is determined predominantly by the properties of the cortical shell at the relevant geometrical constraints. The influence of the transformed cytoskeleton on the cell shape (Boulbitch, 1998) can be understood by considering that cell shape should accommodate the microtubular rod of length L (Emsellem et al., 1998).

We consider the cortical shell to be essentialy composed of two parts: the plasma membrane and the

actin cortex layer (Yeung and Evans, 1989). The actin cortex is a source of the in-plane resting tension (σ_0) because of the contractile elements acting in a tangential direction with respect to the membrane surface. The contractile elements are embedded in the actin cortex layer (Yeung and Evans, 1989). The actin cortex has anisotropic mechanical properties (Yeung and Evans, 1989) contributing to the shear energy (Yeung and Evans, 1989; Evans and Skalak, 1980; Parker and Winlove, 1999) of the cortical shell. On the other hand, the bilayer plasma membrane is usually considered as a two-dimensional liquid material which is highly deformable upon shearing and bending but resists area expansion (Helfrich, 1973; Evans and Skalak, 1980; Schmidt-Schönbein, 1990; Sackmann, 1994; Boulbitch, 1998). It has been shown recently that in the membrane regions with large difference between the two principal curvatures, the plasma membrane may exibit the properties of a two-dimensional liquid crystal due to orientational ordering of the anisotropic membrane constituents (Kralj-Iglič et al., 1999, 2000).

In this work, the apparent area of the cortical shell (A) is defined as the area of the average smooth cortical shell surface where the contribution of the wrinkles and folds is not taken into account explicitly. Therefore, the cortical shell wrinkles and folds serve as reservoir of this defined apparent (projected) membrane area A (Schmidt-Schönbein, 1990). The apparent cortical shell area A may reach its maximal posssible value when the wrinkles are smoothened out completely (Evans and Kukan, 1984; Thoumine et al., 1999). At this point, further increase of the apparent cortical shell area is very difficult since the lipid bilayer plasma membrane shows very large resistance to the change of the area (Evans and Skalak, 1980).

Here, we take for simplicity that the effective tension of the cortical shell (σ) after cytochalasin B treatment is in-plane and isotropic (Thoumine et al., 1999). The shear deformations are not taken into account (Thoumine et al., 1999). This is in our case a reasonable approximation due to degradation of the actin cortex after the cytochalasin B treatment, leaving only clumps of actin attached to the plasma membrane (Fig. 3b). The bending energy is neglected (Yeung and Evans, 1989). Since we study only the equilibrium cell shape we also neglect the cell viscous properties which may play an important role in cell shape transformation at a time scales of minutes (Thoumine and Ott, 1997). Accordingly, we describe the cell cortical shell surface elasticity with the first-order expansion law (Needham and Hochmuth, 1992; Thoumine et al., 1999).

$$\sigma = \sigma_0 + K\alpha, \tag{1}$$

where K is the apparent area expansion modulus and α is the relative change in the apparent surface area. The corresponding area density of the stretching elastic energy can be written as (Evans and Skalak, 1980)

$$E = \sigma_0\alpha + \frac{K}{2}\alpha^2. \tag{2}$$

Combining Eqs. (1) and (2) the total elastic energy of the cell cortical shell $W = \int E\,\mathrm{d}A$ can be expressed as a function of σ as follows

$$W = \frac{1}{2K}\int \sigma^2 - \sigma_0^2\,\mathrm{d}A, \tag{3}$$

where $\mathrm{d}A$ is the area element of the apparent cortical shell.

In the following, the analysis is restricted to axisymmetric cell shapes where the symmetry axis of the cell is the x-axis, so that the shape is given by the rotation of the function $y(x)$ around the x-axis (Fig. 4). The function $y(x)$ is the half-thickness of the cell, i.e., the cell shape has a mirror symmetry with respect to the y-axis (Fig. 4). The shape of the cortical shell which is in close contact with the tip of the microtubular rod is defined by the local configuration of the microtubular rod (Fig. 5). The direction of the x-axis coincides with the direction of the rigid rod-like microtubule structure of length L and width D within the cell. This structure pushes the cortical shell with the axial resultant force F (Fig. 5) at both poles of the cell (Fig. 4).

The resultant force F (Fig. 5) must be balanced by the effective tension σ at any transverse section (Evans and Skalak, 1980)

$$F = \sigma\cos\vartheta\, 2\pi y, \tag{4}$$

where the meaning of the angle ϑ is defined in Fig. 5. By taking into account Eq. (4), $\mathrm{d}A = 2\pi(1+y'^2)^{1/2}y\,\mathrm{d}x$ and $\cos\vartheta = (1+y'^2)^{-1/2}$ the cortical shell elastic energy W (Eq. (3)) can be written in the form

$$W = (F^2/2\pi K)\int_0^{L/2}(1+y'^2)^{3/2}y^{-1}\,\mathrm{d}x. \tag{5}$$

In the following, the cell shape is parametrized by a polynomial function in the form

$$y(x) = a(1+cx^3)^{-n} + d. \tag{6}$$

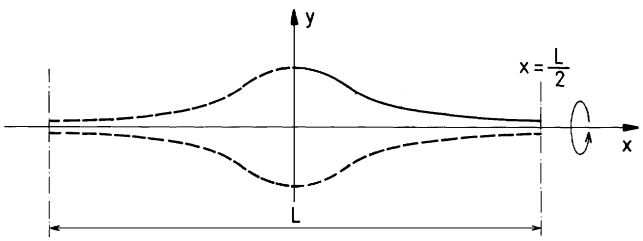

Fig. 4. The coordinates in the cell contour simulation. The axisymmetric cell shape is formed by the rotation of the curve $y(x)$ (full line) about the x-axis for positive x. The cell shape has the mirror symmetry with respect to the y-axis. The rod of the microtubules with the length L and the width D (Fig. 5) extends within the cell between two poles at $x = -L/2$ and $x = +L/2$. The value of y at $x = L/2$ is equal to the half of the thickness of the microtubular rod, i.e., $D/2$ (see also Fig. 5).

The distance between the two poles of the cell shape is equal to the length of the microtubular rod L (Fig. 4). The function $y(x)$ contains four free parameters a, c, n and d. The formulation of the function $y(x)$ contains sufficient number of free parameters so that the contour could be varied seeking for the minimum of the cortical shell energy W within the constraints of fixed cell area and volume and the boundary condition at the tip of the cell, $y(x = L/2) = D/2$ (Figs. 4 and 5).

The equilibrium cell shape described by the function $y(x)$ at given cell area (A), volume (V), length (L) and width of the microtubular rod (D) is therefore obtained by the minimization of the elastic energy W. In this procedure, the parameter d as a function of parameters a, c, n is determined from the boundary condition $y(x = L/2) = D/2$ (Fig. 5). Then the parameters a and n as functions of the parameter c are determined numerically from the constraints for the cell volume

$$V = 2\int_0^{L/2} \pi y^2 \mathrm{d}x \tag{7}$$

and surface area

$$A = 2\int_0^{L/2} 2\pi(1 + y'^2)^{1/2} y \,\mathrm{d}x. \tag{8}$$

The remaining parameter c is then determined by the minimization of the energy W (Fig. 6). In these calculations a, c, d, L, D, x and y are considered to be dimensionless quantities. Consequently, also A and V are dimensionless. The integrals in Eqs. (5), (7) and (8) are calculated numerically using the trapezoidal formula.

Fig. 7 shows the dependence of the equilibrium cell shape on the apparent cell area A at fixed length of the microtubular rod and fixed cell volume V. It can be seen

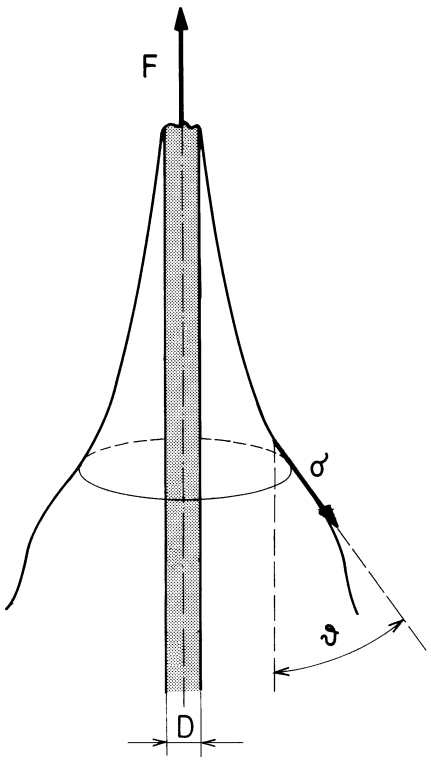

Fig. 5. The geometrical and mechanical parameters determining the cell shape. The shape of the cortical shell which is in the close contact with the tip of the microtubular rod is determined by the local configuration of the microtubular rod.

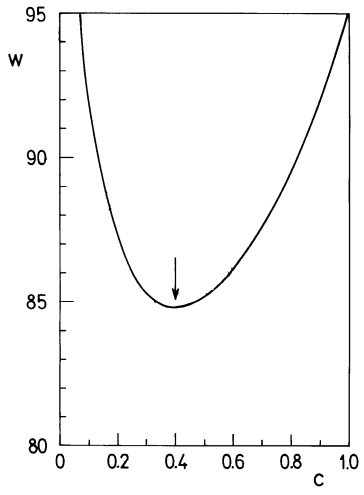

Fig. 6. The relative energy $w = W/(F^2/2\pi K)$ as a function of the parameter c for $A = 23.5$, $V = 8.7$, $L = 10$, $\sigma_0 = 0$ and $D = 0.04$.

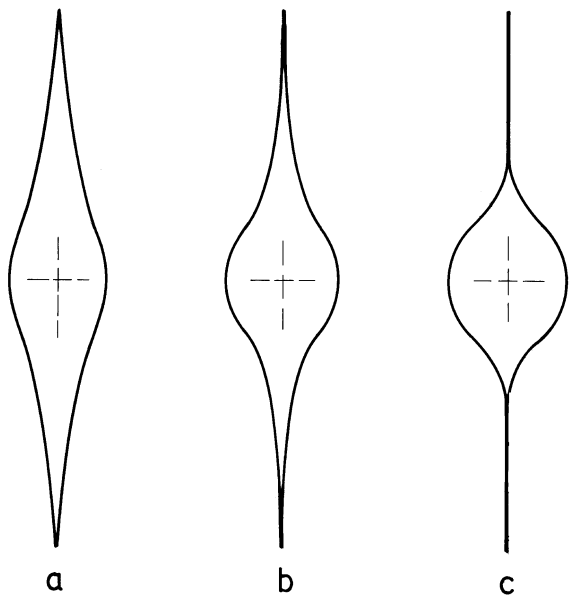

Fig. 7. The calculaled equilibrium cell shape as a function of the decreasing apparent cell surface area A: 26.5 (a), 23.5 (b) and 21.0 (c) at fixed cell volume $V = 8.05$ and fixed length of the rigid microtubular rod $L = 10$. The thickness of the microtubular rod is $D = 0.04$.

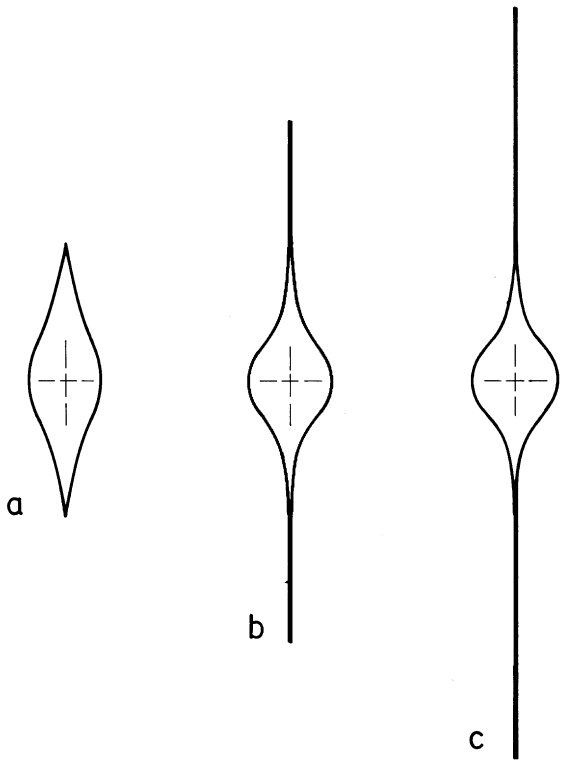

Fig. 8. The equlibrium cell shapes calculated for three values of the length of the microtubular rod inside the cell (L): 7.2 (a), 13.6 (b) and 20.0 (c). The apparent cell area $A=23.5$ and the cell volume $V=8.05$ are the same for all three calculated shapes. The thickness of the microtubular rod is $D=0.04$.

in Fig. 7 that the central part of the equilibrium cell shape becomes increasingly spherical while both arms simultaneously become thinner and more tube-like with decreasing apparent cell surface area A. It can be concluded that at fixed V and L, the calculated cell shapes more and more resemble the ϕ shape with decreasing cell area A.

To illustrate the effect of the length of the microtubular rod (L) inside the cell, on the equlibrium cell shapes, Fig. 8 shows the calculated equlibrium cell shapes as a function of the rod length at fixed cell area A and volume V. With increasing length of the rod L the central part becomes more spherical while the thin arms become more tubular, i.e., the cell shape approaches the ϕ shape.

5. Conclusions and discussion

We have shown that disaggregation of actin filaments after the cytochalasin B treatment induced the formation of the cell shape resembling the Greek letter ϕ . The observed cell shape transformation is accompanied by degradation of actin cortex leaving only clumps of actin attached to the bilayer membrane as well as by large reduction of the attachment area of the cell. The reduction of the contact (adhesion) area between the cell and the substrate is strongly related to the disconnection of the focal contacts. The disconnection is a consequence of disintegration of stress fibers which are crucially involved in functioning of the focal contacts (Jockusch et al., 1995).

It follows from Eq. (4) that the much higher tension $\sigma = F/(\cos\vartheta\, 2\pi y)$ in the regions of the cell protrusions compared with the rest of the cell is due to a smaller value of y. On the basis of this result, one would expect that the surface of the cell protrusion would be more smooth due to higher tension σ having less wrinkles and folds compared to the surface of the cell body. This theoretical conclusion is in good agreement with the observations presented in Fig. 1b.

Cytochalasin B has no direct effect on microtubules (Ostlund et al., 1980). However, upon disaggregation of the actin filaments, the microtubules are reorganized, as their interactions with surrounding structures are changed. It was suggested in this work that this reorganization of the microtubules into the microtubular rod may induce the cell shape transformation driven by the minimization of the cortical shell elastic energy. It was shown theoretically that the calculated equilibrium cell shape corresponding to the minimum of the cortical shell stretching elastic energy becomes more like the ϕ shape with decreasing apparent cell area A (Fig. 7) and increasing length of the microtubular rod (Fig. 8). A related effect has been observed in the case of phospholipid vesicles with a microtubular rod (Elbaum et al., 1996; Fygenson et al., 1997; Emsellem et al., 1998; Umeda et al., 1998), where the tubulin, encapsuled by the vesicles, polymerized and assembled into a rod within the vesicles. The rod grew and increased in length, causing the transformation of the initially ellipsoid vesicle into the shape that had a ϕ profile. The effect of the microtubule rod on the vesicle shape has been theoretically described by taking into account the elastic properties of the bilayer membrane and appropriate geometrical constraints as for example constraints for the vesicle volume and the length of the rod (Fygenson et al., 1997; Emsellem et al., 1998; Umeda et al., 1998).

On the basis of the similarity between the ϕ shape of V-79 cells with long tubular protrusions containing a microtubular rod and the ϕ shape of the phospholipid vesicles with a long entrapped microtubular rod we suggest that some common simple physical mechanisms take place in both cases. It seems that at sufficiently large relative cell (vesicle) volumes $v=(36\pi V^2)^{1/2}/A^{3/2}$ (Iglič et al., 1999), the observed ϕ shape of V-79 cells after cytochalasin B treatment and of phospholipid vesicles with long entrapped rod ($L\gg(A/4\pi)^{1/2}$), is mainly dictated by the geometrical constraints for V and

A. Namely, in these cells (vesicles) nearly all the volume should be enclosed in a central spherical or ellipsoidal part while the contributions of the arms to V and A should be as small as possible. In accordance, it was observed that in the V-79 cells where the cytochalasin B treatment was followed by the colchicine treatment that induced the complete disorganization of microtubular rod, the characteristic ϕ shape disappeared.

The results of this work may be relevant also for explanation of the cell shape under physiological conditions. In the normal mammalian red blood cells which have no internal structure, the cell shape is determined solely by the cell membrane (Evans and Skalak, 1980; Sackmann, 1994; Iglič 1997; Parker and Winlove, 1999) which is essentialy composed of two parts, the bilayer and the underlaying membrane skeleton. In most of the other cells, the cytoskeleton is the principal determinant of the cell shape (Gupta et al., 1996; Ingber et al., 1995) where the coupling between the cortical shell and the cell nucleus provided by the cytoskeleton plays an important role (Ingber, 1997). For example, in fish red blood cells the cell shape seems to be mainly dictated by the three-dimensional cytoskeletal system (including marginal band of microtubules and the intermediate filaments) connecting the cell membrane and the nucleus (Hägerstrand et al., 2000). In the hereditary human disease sickle-cell anemia, the rodlike structure of polymerized hemoglobin S in the sickled red blood cells induces a formation of similar shapes with long tubular spicules on the cell surface (Liu et al., 1991) as shown in Figs. 7 and 8. Also, the shape of thin tubular membrane extensions distributed over the cell surface (filopodia) which are provoked by long rodlike structures of the cytoskeleton (Gupta et al., 1996; Sit, 1996; Cooper, 2000) might be at least partly explained by the cell surface area and energy constraints at a given volume of the cell.

Acknowledgements

The authors would like to thank Alexei A. Boulbitch, Henry Hägerstrand and Virginie Emsellem for fruitful and stimulating discussions.

References

Alberts, B., Bray, D., Lewis, J., Raff, M., Roberts, K., Watson, J.D., 1994. Molecular Biology of the Cell, Garland Publishing Inc., New York, pp. 787–846.

Bell, P.B., Safiejko-Mroczka, B., 1995. Improved methods for preserving macromolecular structures and visualizing them by fluorescence and scanning electron microscopy. Scanning Microscopy 9, 843–860.

Boulbitch, A.A., 1998. Deflection of a cell membrane under application of local force. Physical Review E 57, 1–5.

Cooper, G.M., 2000. The Cell. A Molecular Approach, ASM Press, Washington DC, pp. 1–689.

Elbaum, M., Fygenson, D.K., Libchaber, A., 1996. Buckling microtubules in vesicles. Physical Review Letters 76, 4078–4081.

Emsellem, V., Cardoso, O., Tabeling, P., 1998. Vesicle deformation by microtubules: a phase diagram. Physical Review E 58, 4807–4810.

Evans, E., Kukan, B., 1984. Passive material behaviour of granulocytes based on large deformation and recovery after deformation tests. Blood 64, 1028–1035.

Evans, E., Skalak, R., 1980. Mechanics and Thermodynamics of Biomembranes, CRC Press Inc., Boca Raton, FL, pp. 1–254.

Fygenson, D.K., Marko, J.F., Libchaber, A., 1997. Mechanics of microtubule based membrane extension. Physical Review Letters 79, 4497–4500.

Gupta, P.D., Nandini, R., Rao, K.S., 1996. Hormone-induced changes in cell shape: role of cytoskeletal proteins. Cytobiosis 86, 75–111.

Hägerstrand, H., Danieluk, M., Bobrowska-Hägerstrand, M., Iglič, A., Wrobel, A., Isomaa, B., Nikinmaa, M., 2000. Influence of band 3 protein absence and skeletal structures on amphiphile and Ca^{2+} induced shape alterations in erythrocytes: a study with lamprey (*Lampetra fluviatilis*), trout (*Onchorhynchus mykiss*) and human erythrocytes. Biochimica et Biophysica Acta 1466, 125–138.

Helfrich, W., 1973. Elastic properties of lipid bilayers: theory and posssible experiments. Zeitschrift für Naturforschung 29C, 693–703.

Iglič, A., 1997. A possible mechanism determining the stability of spiculated red blood cells. Journal of Biomechanics 30, 35–40.

Iglič, A., Kralj-Iglič, V., Majhenc, J., 1999. Cylindrical shapes of closed bilayer structures correspond to an extreme area difference between the two monolayers of the bilayer. Journal of Biomechanics 32, 1343–1347.

Ingber, D.E., 1997. Tensegrity: the architectural basis of cellular mechanotransduction. Annual Review of Physiology 59, 575–599.

Ingber, D.E., Prusty, D., Sun, Z., Betensky, H., Wang, N., 1995. Cell shape, cytoskeletal mechanics, and cell cycle control and angiogenesis. Journal of Biomechanics 28, 1471–1484.

Jockusch, B.M., Bubeck, P., Giehl, K., Kroemker, M., Moschner, J., Rothkegel, M., Rudiger, M., Schluter, K., Stanke, G., Winkler, J., 1995. The molecular architecture of focal adhesions. Annual Review of Cell and Developmental Biology 11, 379–416.

Kralj-Iglič, V., Heinrich, V., Svetina, S., Žekš, B., 1999. Free energy of closed membrane with anisotropic inclusions. European Physical Journal B 10, 5–8.

Kralj-Iglič, V., Iglič, A., Hägerstrand, H., Peterlin, P., 2000. Stable tubular microexovesicles of the erythrocyte membrane induced by dimeric amphiphiles. Physical Review E 61, 4230–4234.

Liu, S.C., Derick, L.H., Zhai, S., Palek, J., 1991. Uncoupling of the spectrin-based skeleton from the lipid bilayer in sickled red cells. Science 252, 574–576.

Needham, D., Hochmuth, R.M., 1992. A sensitive measure of surface stress in the resting neutrophil. Biophysical Journal 61, 1664–1670.

Ostlund, R.E., Leung, J.T., Hajek, S.V., 1980. Regulation of microtubule assembly in cultured fibroblast. Journal of Cell Biology 85, 386–391.

Parker, K.H., Winlove, C.P., 1999. The deformation of spherical vesicle with permeable, constant-area membranes : application to the red blood cell. Biophysical Journal 77, 3096–3107.

Sackmann, E., 1994. Membrane bending energy concept of vesicle and cell shapes and shape transitions. FEBS Letters 346, 3–16.

Schmidt-Schönbein, G.W., 1990. Leukocyte biophysics. Cell Biophysics 17, 107–135.

Sit, K.H., 1996. Cell rounding with rip off detachment. Histology and Histopatology 11, 215–227.

Thoumine, O., Cardoso, O., Meister, J.J., 1999. Changes in the mechanical properties of fibroblasts during spreading: a micromanipulation study. European Biohysics Journal 28, 222–234.

Thoumine, O., Ott, A., 1997. Time scale dependent viscoelastic and contractile regimes in fibroblasts probed by microplate manipulation. Journal of Cell Science 110, 2109–2116.

Umeda, T., Nakajima, H., Hotani, H., 1998. Theoretical analysis of shape transformations of liposomes caused by microtubule assembly. Journal of the Physical Society of Japan 67, 682–688.

Yeung, A., Evans, E., 1989. Cortical shell-liquid core model for passive flow of liquid-like spherical cells into micropipets. Biophysical Journal 56, 139–149.